Separation Science and Technology
Publication details, including instructions for authors and subscription information:
http://www.informaworld.com/smpp/title~content=t713708471

NEW MAGNETIC FIELD-ENHANCED PROCESS FOR THE TREATMENT OF AQUEOUS WASTES

Armin D. Ebner[a]; James A. Ritter[a]; Harry J. Ploehn[a]; Robert L. Kochen[b]; James D. Navratil[c]
[a] Department of Chemical Engineering, Swearingen Engineering Center, University of South Carolina, Columbia, SC [b] Rocky Flats Environmental Technology Site, Golden, CO [c] Lockheed Martin Technologies Company, Idaho Falls, ID

To cite this Article Ebner, Armin D. , Ritter, James A. , Ploehn, Harry J. , Kochen, Robert L. and Navratil, James D.(1999) 'NEW MAGNETIC FIELD-ENHANCED PROCESS FOR THE TREATMENT OF AQUEOUS WASTES', Separation Science and Technology, 34: 6, 1277 — 1300
To link to this Article: DOI: 10.1080/01496399908951093
URL: http://dx.doi.org/10.1080/01496399908951093

SEPARATION SCIENCE AND TECHNOLOGY, 34(6&7), pp. 1277–1300, 1999

NEW MAGNETIC FIELD–ENHANCED PROCESS FOR THE TREATMENT OF AQUEOUS WASTES

Armin D. Ebner, James A. Ritter* and Harry J. Ploehn
Department of Chemical Engineering
Swearingen Engineering Center
University of South Carolina
Columbia, SC 29208

Robert L. Kochen
Rocky Flats Environmental Technology Site
P.O. Box 464,Golden, CO 80402

James D. Navratil
Lockheed Martin Technologies Company
P.O.Box 1625, Idaho Falls, ID 83415

ABSTRACT

A new magnetic adsorbent material, called magnetic polyamine-epichlorohydrin (MPE) resin, was prepared by attaching activated magnetite to the outer surface of polyamine-epichlorohydrin resin beads. Experiments were carried out in the presence of a 0.3-tesla magnetic field to investigate the removal of actinides (plutonium and americium) from pH 12 wastewater using this new resin. The results demonstrated that the MPE resin has a significantly enhanced capacity for actinides over conventional ferrite-based surface complexation adsorption processes (where no field is applied) and over traditional high-gradient magnetic separation (HGMS) processes that remove suspended particles. This enhancement was attributed to the presence and subsequent removal of suspended actinide nanoparticles through an HGMS effect, with the magnetite acting as a very effective HGMS element. A theoretical analysis verified this supposition by showing that under adequate pHs and particle-particle separations, the attractive long-ranged magnetic force exerted by magnetite on suspended particles of plutonium hydroxide was greater in magnitude than other forces (e.g., van der Waals, electrostatic, viscous, and Brownian forces).

* Author for correspondence. E-mail: ritter@sun.che.sc.edu

INTRODUCTION

High-gradient magnetic separation (HGMS) processes have been used extensively in the processing of minerals (1,2), water treatment, and environmental remediation (3,4), and more recently, in studies for the removal of microorganisms and magnetic particles by magnetic coating (5–7) and magnetic seeding (8–12), respectively. Conventional HGMS processes use a fine stainless steel wool to form a magnetic matrix within a flow field of a solution containing mineral particles to be separated. Ferromagnetic or paramagnetic particles in this solution move in the direction of an increasing magnetic gradient and are attracted to (and stick to) this energized stainless steel mesh. Diamagnetic materials, on the other hand, move in the direction of a decreasing magnetic gradient and are essentially repelled from the mesh. Also, in order for these processes to remove soluble metal species from solution, they must utilize precipitating or flocculating agents to first effect the formation of particles, which must become sufficiently large to make the separation efficient and inexpensive. Although this problem cannot be completely avoided, it may be alleviated somewhat with the use of a new magnetic resin, called magnetic polyamine-epichlorohydrin (MPE) (13,14).

MPE resin consists of spherical beads of polyamine-epichlorohydrin that have activated iron ferrite (magnetite) particles attached to their outer surfaces. Ferrites are a class of mixed-valence iron oxide compounds having the crystal structure of spinel, $MgAl_2O_4$. Iron atoms in iron ferrite ($FeO{\cdot}Fe_2O_3$), or magnetite, can be replaced by many other metal ions (Mn, Co, Ni, Cu, Mg, Zn, etc.) without seriously altering the spinel structure. They can also be activated using a strong base (e.g., barium hydroxide), thereby improving the metal-ion adsorption capacity via interaction with newly formed surface hydroxyl groups (13–14). As a result, ferrites have been shown to be excellent adsorbents for the separation of hazardous metals (cadmium, lead, mercury, etc.) and actinide elements (americium, plutonium, and uranium) from wastewater (15–19) at relatively low alkaline conditions (pH > 9) and independent of a magnetic field.

Under highly alkaline conditions, most metal ions form either precipitates that remain suspended in solution or complexes with the hydroxylated surface of any typical oxide such as ferrites. The latter is typically referred to as metal–ion adsorption. Ferrites are also ferrimagnetic crystalline materials that are soluble only in strong acid; thus, they

can be used in alkaline conditions as a very fine magnetic element in HGMS systems. Thus, the MPE resin has the potential to improve the performance of HGMS systems because of the unique ability of magnetite not only to adsorb metal ions via surface complexation but also to magnetically attract and retain magnetic nanoparticles (suspended precipitates) close to its surface. In fact, Ebner et al. (20) showed recently that because of their size (typically 0.2 μm) and high saturation magnetization (about 4 to 5 times smaller than iron) magnetite particles can create magnetic forces around small paramagnetic colloidal particles (down to 40 nm) that are several times stronger than those created by typical stainless steel wool meshes with wire diameters on the order of 10 μm. Therefore, with the use of the MPE resin, a new magnetic field–enhanced process has been developed, which couples HGMS principles together with surface complexation adsorption.

This paper presents some preliminary experimental results obtained with this new magnetic field–enhanced process using a continuous-flow breakthrough system, the MPE resin, and a dilute actinide solution containing plutonium and americium at pH 12. Comparisons are made with the more conventional HGMS systems and with the more traditional nonmagnetic batch processes that utilize surface complexation (i.e., metal-ion adsorption). A qualitative theoretical analysis for the enhanced effect of the magnetic field on the results is also given.

EXPERIMENTAL

Resin Preparation

MPE resin beads were synthesized with activated ferrite particles attached to the outer surface of the beads (13, 14, 21, 22). This was done in a two-step procedure. In the first step, 1.7 mol (103 g) of aqueous ammonia solution (28 wt %) was placed into a 1-L, three-necked flask equipped with a mechanical stirrer, a thermometer, and a dropping funnel (125 mL). Then 1 mol (92.5 g) of epichlorohydrin was placed into the dropping funnel and added dropwise to the stirred (500-rpm) aqueous ammonia solution. The epichlorohydrin was added over a 1-h period, with the rate of addition being sufficient to maintain an exothermic reaction temperature of 90°C. At the end of the 1-h period, a clear, transparent polymer (ammonia-epichlorohydrin) was removed and cooled to

ambient temperature (23°C). In the second step, 95.0 g of this polymer, 58.0 g of polyethyleneimine (10 wt % aqueous solution), and 9.0 g of wet, activated ferrite (in this case, magnetite) was added to a 1-L, three-necked flask that contained 150 mL of toluene and 4.5 g of Aerosol™ GPG surfactant. The flask was equipped with a heating mantel, a thermometer, a mechanical stirrer, a Friedrichs™ condenser (350 mm), and a Dean & Stark™ water trap (20 mL).

This mixture was stirred for 5 min (1700 rpm), and then an additional 5 g of epichlorohydrin was added to the flask. The temperature was then raised to 85°C, and the azeotropic mixture of water and toluene was stirred (1000 rpm) under total reflux. Additional toluene (350 mL) was added as needed. The refluxing was continued for 4.5 h, and the water was removed, as necessary, from the Dean & Stark™ trap. At the end of the heating period, the MPE resin product was cooled, filtered through Whatman No. 41 (20- to 25-μm) filter paper, air dried, and sieved.

MPE resin synthesized according to this procedure contained approximately 8 wt % magnetite (i.e., 80 mg of magnetite per gram of resin). Nonmagnetic, polyamine-epichlorohydrin resin (PE) was also synthesized following this same procedure, but without adding magnetite. Results are reported based on both types of resins, MPE and PE, to emphasize the unique properties and capabilities of the magnetite.

Resin Characterization

The synthesis procedure given above for the MPE resin produced highly spherical particles that ranged in size from 0.063 to 0.125 mm in diameter. Scanning electronmicrographs of the MPE resin are shown in Figures 1–3. The highly spherical nature of the beads is very apparent in these photographs. Moreover, Figure 2 shows that the surface of the beads was very rough, containing many small indentations. It was first thought that these indentations were the entrances to a large network of internal pores; however, the nitrogen BET surface area of the MPE resin was less than 1 m^2/g, indicating that the beads were nonporous. Figure 3 shows another scanning electronmicrograph of the MPE resin taken at a much higher magnification. The surface roughness was primarily due to magnetic particles attached to the outer surface of the beads, with individual particles being about 0.1 μm in diameter and clusters of particles ranging from

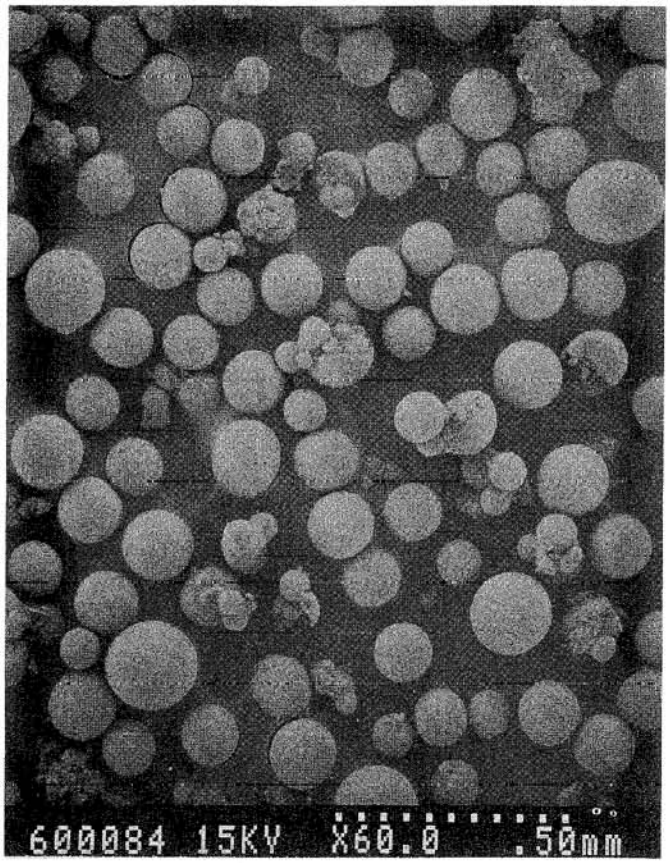

FIGURE 1. Scanning electronmicrograph of many MPE resin beads.

1 to 4 μm. These small particles of magnetite were verified using elemental dispersive X-ray analysis, and X-ray diffraction. Figure 4 compares the XRD pattern from the MPE resin with that from pure magnetite, which shows that the MPE synthesis procedure did not alter the crystal structure of the magnetite when attached to the surface of the resin.

Column Preparation

The upper portion of a glass, chromatographic column (19 mm ID x 25 cm) was packed with a small plug of glass wool and a 10-cm plug of fine, No. 431 stainless steel

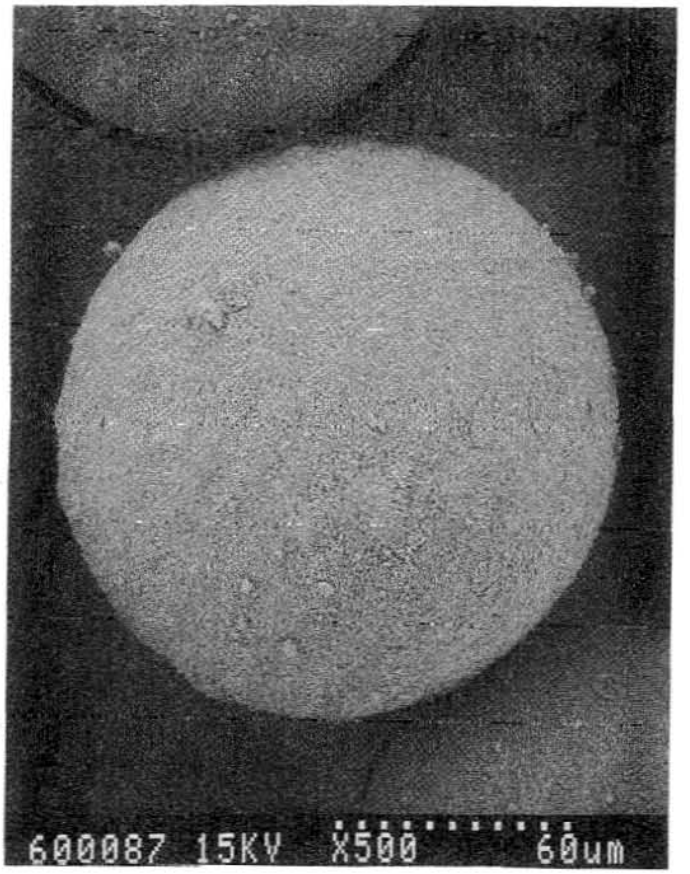

FIGURE 2. Scanning electronmicrograph of a single MPE resin bead.

wool and placed (with the bottom portion of the stainless steel wool) between the pole faces of an electromagnet. The bottom and top of the column were fitted with a stop-cock and rubber stopper with an exit tube, respectively. Tygon tubing was attached to both ends of the column. The experimental setup is shown in Figure 5.

Next, the magnetic (MPE) resin was activated (16) by stirring the resin with a solution of barium hydroxide (2.6 mmol per gram of magnetite) for 10 min at ambient temperature. The excess barium hydroxide solution was then decanted, and sodium

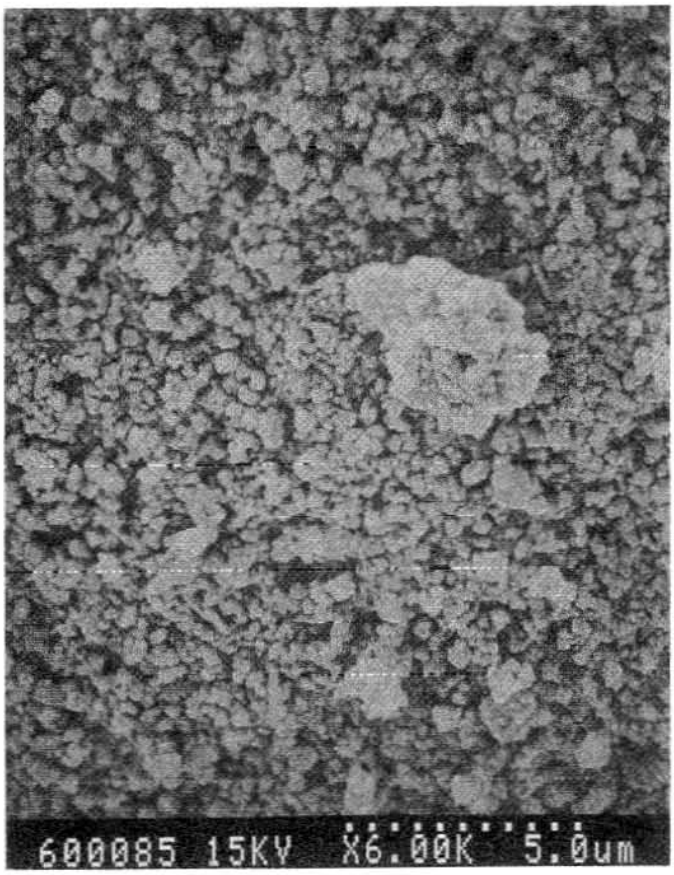

FIGURE 3. Scanning electronmicrograph of the surface of an MPE resin bead.

hydroxide solution (pH 12.0) was added to the wet resin. The resulting slurry was then pumped (upflow at 10 mL/min via a peristaltic pump) into the glass column with the electromagnet energized and generating a field strength of approximately 0.5 T (or 5000 gauss). The MPE resin was retained in the column by the steel and glass wool plugs. The column was now ready for use.

For a typical experiment with simulated wastewater (deionized water spiked with americium and plutonium ions, pH adjusted to 12 with a sodium hydroxide solution, and

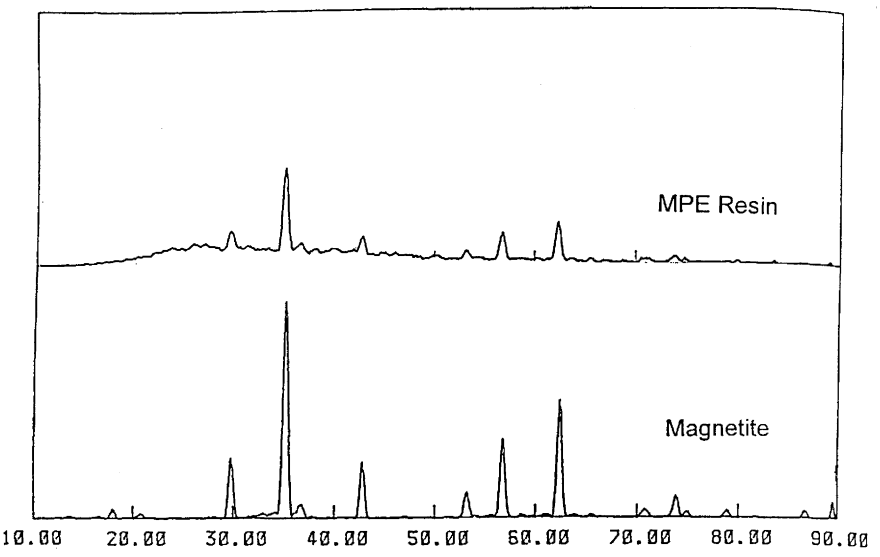

FIGURE 4. Comparison between X-ray diffraction patterns of MPE resin and pure magnetite.

prepared fresh before each experiment), the magnet was energized, which created a magnetic field strength of approximately 0.3 T. The solution containing the actinide species was then pumped through the column (upflow at a specified flow rate, see below), and effluent fractions were collected and monitored radiometrically by alpha (plutonium) and gamma (americium) counting. The results were plotted as a function of time (plotted in this work as the volume of effluent that was passed through the column) until the actinide species began to break through the column. At this point, the experiment was completed.

THEORETICAL

A magnetic heteroflocculation model was developed that considers different colloidal forces that exist between a free-moving plutonium particle of radius R_p and a stationary magnetite particle of radius R_s. The net force between these two particles was comprised

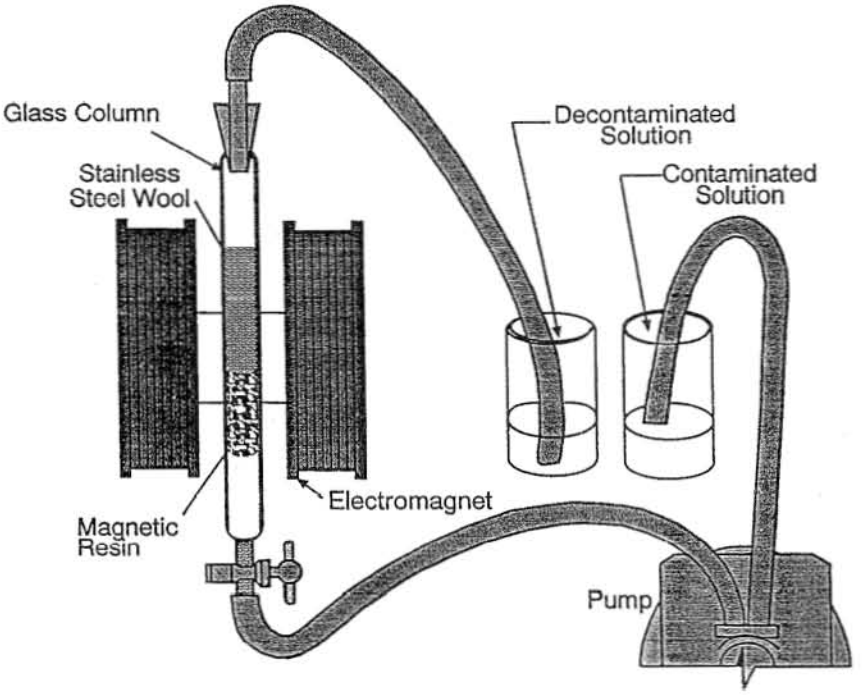

FIGURE 5. Fixed-bed HGMS apparatus used in the MPE and PE breakthrough experiments.

of van der Waals, electrostatic, magnetic, and Brownian forces. This net force was also compared with the viscous force in the Stokes flow regime, which is the regime where the breakthrough experiments were carried out. Additional details of the model and its complete development are given elsewhere (23). The physical properties used in this model are given in Table 1.

Viscous Forces

The modulus of the viscous or drag force, F_d, over a free-moving particle of plutonium was estimated using Stokes' law, which is given by

$$F_d = 6\pi\mu R_p v, \quad (1)$$

TABLE 1. PHYSICAL PROPERTIES USED IN THE MAGNETIC HETEROFLOCCULATION MODEL

$Pu(OH)_4$ volumetric susceptibility, χ_p	:	8.0×10^{-4}
Magnetite saturated magnetization, $M_{s,m}$	:	4.8×10^{-5} A m^{-1}
Medium (water and matrix)[a] susceptibility, χ_m	:	-1.3×10^{-6}
Permeability of free space, μ_o	:	$4\pi \times 10^{-7}$ H m^{-1}
Superficial velocity, v_s	:	3.5 cm min^{-1}
Bed porosity, ε	:	0.4
Liquid viscosity, μ	:	0.001 kg m^{-1} s^{-1}
Hamaker's constant, A	:	5.0×10^{-20} J
Relative permittivity of the medium, ε	:	78.0
Permittivity of free space, ε_o	:	8.85×10^{-12} F m^{-1}

[a] The MPE resin was assumed to have the same susceptibility as water.

where μ is the dynamic viscosity and v is the free stream interstitial velocity or v_s/ε, where v_s is the superficial velocity and ε is the bed porosity. It must be emphasized that the convective forces calculated from Equation (1) were probably overestimated because they were based on the interstitial velocity of the free stream. Boundary layers and stagnant regions definitely existed around the MPE particles; thus, when the plutonium particle was moving very close to the surface of an MPE bead, the velocity of the fluid and, therefore, the actual F_d were expected to be much less.

van der Waals Forces

The van der Waals force exerted by a magnetite particle on a plutonium particle when they are separated by a distance h (surface to surface) was derived from Hamaker's formula (24), which is given by

$$\mathbf{F}_w = -\frac{A(16\lambda)^3}{3(R_p + R_s)}\left[\frac{s}{(1+\lambda)^2(s^2-4)^2(s^2(1+\lambda)^2 - 4(1-\lambda)^2)^2}\right]\mathbf{e}_r, \qquad (2)$$

where

$$s = 2\frac{h + R_p + R_s}{R_p + R_s}, \tag{3}$$

$$\lambda = \frac{R_s}{R_p}, \tag{4}$$

and A is Hamaker's constant.

Electrostatic Forces

Hogg et al. (25) used the Derjaguin method to obtain an approximate electrostatic interaction energy and force between two dissimilar spheres when their sizes were large in comparison to the thickness of the double layer and the separation between the spheres. When constant surface charge is assumed as a boundary condition for the diffuse layer, the electrostatic force, $\mathbf{F}_e$, exerted by a magnetite particle on a plutonium particle is expressed as

$$\mathbf{F}_e = 4\pi\varepsilon_r\varepsilon_o\kappa G_{ps}\frac{e^{-h\kappa}}{1-e^{h\kappa}}((\psi_s^2 + \psi_p^2)e^{-h\kappa} + 2\psi_s\psi_p)\mathbf{e}_r, \tag{5}$$

where

$$G_{ps} = \frac{R_p R_s}{2(R_p + R_s)}, \tag{6}$$

$$\kappa = \left(\frac{2Ie^2}{\varepsilon_r\varepsilon_o kT}\right)^{0.5}, \tag{7}$$

ψ_s and ψ_p are the infinite separation potentials for each of the particles, which were obtained from the Poisson-Boltzmann equation for single spheres and the constant charge condition, I is the ionic strength of the solution, and ε_r and ε_o are the relative permittivity of the medium and the permittivity of free space, respectively.

Magnetic Forces

According to Ebner et al. (20), the magnetic force, $\mathbf{F}_m$, exerted by a static magnetite sphere on a plutonium particle with susceptibility χ_p and volume V_p is given by

$$\mathbf{F}_m = -\frac{V_p}{2}\mu_o(\chi_p - \chi_m)\nabla(H^2), \tag{8}$$

where χ_m is the susceptibility of the medium, which was considered negligible. The local magnetic field, H, with components in spherical coordinates is given by

$$H_r = \left(H_a + \frac{R_s^3}{3r^3} M_{s,m} \right) \cos\theta , \tag{9}$$

$$H_\theta = \left(-H_a + \frac{R_s^3}{3r^3} M_{s,m} \right) \sin\theta , \tag{10}$$

where $M_{s,m}$ is the saturation magnetization of the magnetite particles and H_a is the magnitude of the applied magnetic field. In this work, the magnetic forces were evaluated in the direction of the external magnetic field (i.e., at $\theta = 0$).

Brownian Forces

The aforementioned forces were only important if their magnitude was substantially greater than the effective Brownian force associated with random thermal motion. The Peclet number (Pe) represents the ratio of the magnitude of any force to the Brownian force and is given by (20)

$$Pe_i = \pm \frac{R_p |\mathbf{F}_i|}{kT}, \tag{11}$$

where k is the Boltzmann constant and T is the absolute temperature. By definition, Pe was taken as negative when the force was attractive and positive when the force was repulsive. The subscript i represents the nature of the force under consideration, which dominates when $|Pe_i| \gg 1$; otherwise, random thermal motion overwhelms any tendency toward particle retention. Consequently, Pe was viewed as the degree of attraction of the species under study; thus, when $Pe_i < -10$, the force i was considered to be strong enough to attract and retain particles, whereas when $Pe_i > 10$ the force i was considered to be strong enough to repel particles.

RESULTS AND DISCUSSION

Breakthrough Experiments with MPE and PE Resin

Twenty grams of MPE resin (particle size range of 0.063 to 0.125 mm) were evaluated for actinide (plutonium and americium) removal from water at a pH of 12.0

(column mode). The breakthrough curves are shown in Figures 6 and 7 for plutonium and americium, respectively. A total of 341 L of actinide solution (1.28×10^{-4} g/L ^{239}Pu and 3.57×10^{-7} g/L ^{241}Am) was processed through the MPE resin bed (upflow) at 3.5 mL min^{-1} cm^{-2} (0.87 gpm/ft^2) with the magnetic field turned on and set at 0.3 T. The column effluent was then filtered through Whatman No. 41 (20- to 25-μm) filter paper to ensure complete removal of the MPE resin particles.

The results showed that the plutonium and americium concentration in 325 L of actinide solution were decreased to 2.77×10^{-8} g/L and 7.17×10^{-10} g/L, respectively, before the plutonium activity in the effluent started to increase. This translates to 4.16×10^{-2} g of plutonium and 1.16×10^{-4} g of americium removed from 325 L of water. Therefore, 8550 L of contaminated water can be treated with 1 L of MPE resin.

For comparative purposes, the polyamine-epichlorohydrin (PE) resin (without magnetite) was also evaluated for actinide removal from water at a pH of 12.0 (column mode). Breakthrough curves for both the PE and the MPE resins are shown in Figure 8. Note that the PE and MPE columns were prepared and operated in a similar fashion. A total of three liters of actinide solution (9.42×10^{-5} g/L ^{239}Pu and 1.10×10^{-7} g/L ^{241}Am) was pumped (upflow) through 20 g of the PE resin (particle size range of 0.063 to 0.125 mm) at 3.5 mL min^{-1} cm^{-2} (0.87 gpm/ft^2) with the magnetic field turned on and set at 0.3 T. The column effluent was then filtered through Whatman No. 41 (20- to 25-μm) filter paper to ensure complete removal of the PE resin particles.

The results showed that the plutonium and americium concentration in 2.75 L of actinide solution were decreased to 5.16×10^{-8} g/L and 5.27×10^{-10} g/L, respectively, before the activity in the column effluent started to increase. Although the minimum concentrations observed for plutonium and americium were comparable to those for the MPE resin, breakthrough occurred two orders of magnitude sooner. This is equivalent to treating only 72 L of contaminated water with 1 L of PE resin, a significantly reduced capacity as compared with the MPE resin. Such results showed that the nonmagnetic PE resin and, more importantly, the stainless steel wool contributed very little to the significant loading capacity exhibited by the MPE resin. Clearly, the magnetite was responsible for the observed trends, which showed a marked improvement with the new magnetic field–enhanced process over the traditional HGMS process.

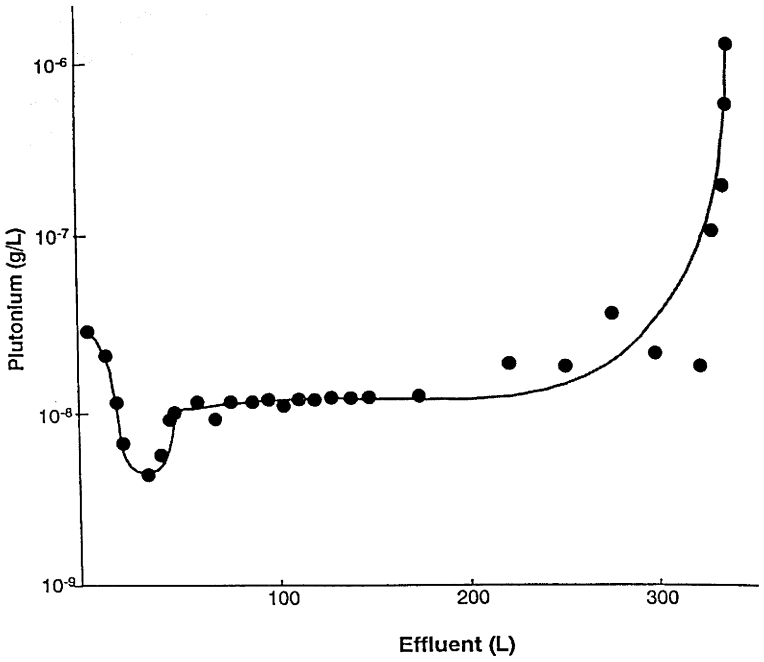

FIGURE 6. Breakthrough curve for plutonium using 20 g of MPE resin, 0.3-T magnetic field, pH 12 simulated wastewater containing 1.28×10^{-4} g/L ^{239}Pu and 3.57×10^{-7} g/L ^{241}Am, and fed upflow at 3.5 mL min^{-1} cm^{-2}.

Effect of the Magnetic Field

The marked improvement in the new magnetic field–enhanced process was attributed mainly to the effect of large magnetic forces in the proximity of the magnetite particles and, to a lesser extent, the surface complexation chemistry of magnetite. To compare the relative importance of these two mechanisms, the electromagnet was energized for a short period of time and deenergized for a short period of time, while passing a few liters of actinide solution through the column. The conditions for this experiment were the same as those used previously with the MPE resin. Samples of the column effluent were also filtered through Whatman No 41 (20- to 25-μm) filter paper and analyzed to ensure complete removal of the resin particles. The effluent profile from this experiment is shown in Figure 9.

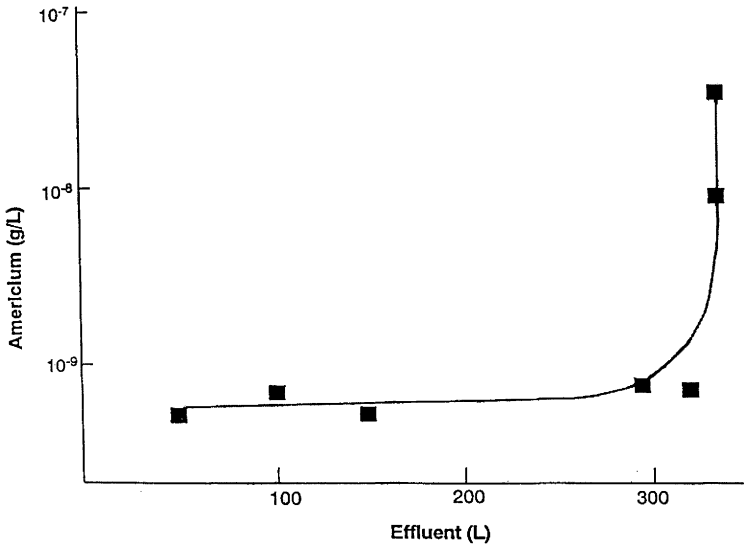

FIGURE 7. Breakthrough curve for americium using 20 g of MPE resin, 0.3-T magnetic field, pH 12 simulated wastewater containing 1.28×10^{-4} g/L ^{239}Pu and 3.57×10^{-7} g/L ^{241}Am, and fed upflow at 3.5 mL min^{-1} cm^{-2}.

Clearly, the external magnetic field had a profound effect on the throughput of the MPE resin. While the magnet was energized, the plutonium concentration in the effluent decreased rapidly by two and one-half orders of magnitude during the time that 3.5 L of solution was passed through the column. When the magnetic field was turned off, the plutonium concentration began to increase rapidly during the time which 1.5 L of solution was passed through the column, generating a nearly symmetric profile about the time the field was turned off. This result not only demonstrated the reversibility of the MPE resin, but more importantly, it revealed the principal phenomenon that was taking place. Under the alkaline conditions of these experiments, plutonium and americium were present mainly as colloidal nanoparticle suspensions (26); and as a result of their paramagnetic properties, they were strongly attracted to and retained by the magnetite particles. This supposition is demonstrated qualitatively with results from the magnetic heteroflocculation model that are shown in Figures 10 and 11.

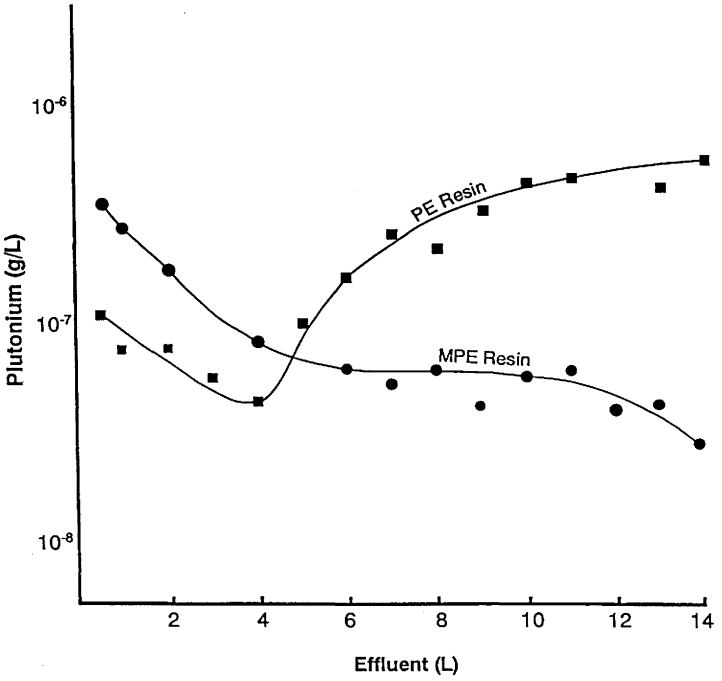

FIGURE 8. Breakthrough curves of the PE and MPE resins using 20 g of PE resin and 20 g of MPE resin, 0.3–T magnetic field, pH 12 simulated wastewater containing 1.28×10^{-4} g/L ^{239}Pu and 3.57×10^{-7} g/L ^{241}Am, and fed upflow at 3.5 mL min^{-1} cm^{-2}.

Figure 10 shows the effects of the charge density and the applied magnetic field on the net dimensionless force (resultant Pe of the magnetic, electrostatic, and van der Waals forces) as a function of the distance between the surfaces of a magnetite particle (R_s = 400 nm) and a plutonium particle with (a) R_p = 160 nm and (b) R_p = 300 at an electrolyte concentration of 0.01 *M* (or pH = 12, if the electrolyte is purely alkaline). Due to the difficulty of experimentally determining the values of the charge densities of diffuse layers in colloidal systems, the range of the values used here was based on estimations obtained from a triple-layer complexation model (27–31). It suffices to state that σ = 0.01 C/m^2 was considered to be relatively high for diffuse layers, since colloidal systems form fixed Stern and Helmholtz layers that prevent diffuse layers from becoming densely charged. Nevertheless, it is clear that the effect of the charge density on the net

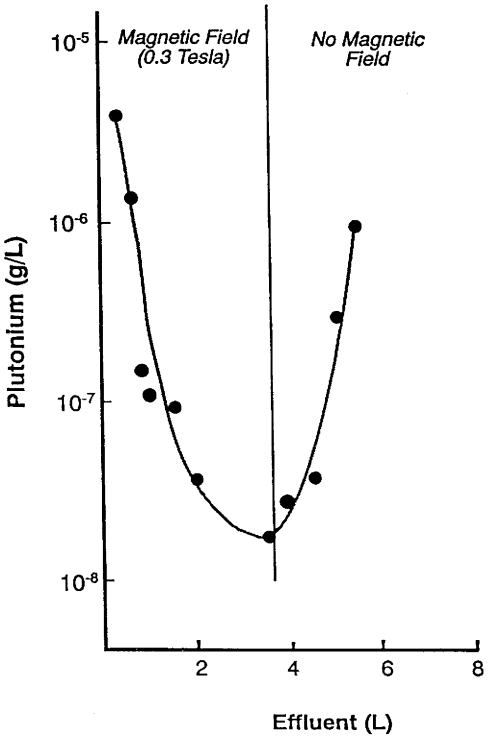

FIGURE 9. Effluent profile for plutonium during an ON/OFF magnetic field experiment at the same conditions as those given in Figure 6 or 7.

force was dramatic. When the two particles were very close (i.e., surface-to-surface distances of less than 5 nm) the electrostatic force became very important, resulting in a very repulsive force. Also, the effect of the applied magnetic field became much more important with larger plutonium particles. For the 160-nm plutonium particle, the effect of the change in the magnetic field was almost negligible. For the 300-nm plutonium particle, however, the effect became significant, although it was still not strong enough to overcome the repulsive electrostatic force.

Figure 11 shows the net dimensionless force (Pe) for larger separations between the same particles and for electrolyte concentrations of 0.01 *M* (or pH =12) and 0.001 *M* (or pH = 11), respectively. The viscous or drag forces (F_d) are also reported in these figures.

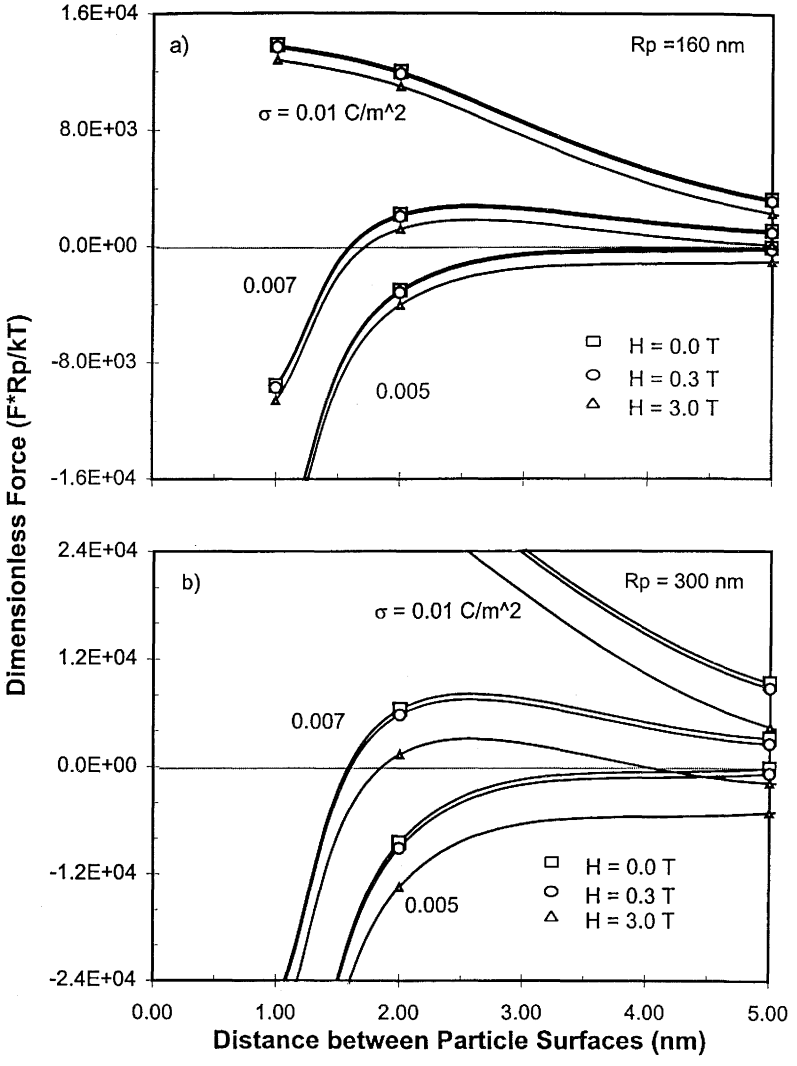

FIGURE 10. Net dimensionless force (Pe) between magnetite (R_s = 400 nm) and a plutonium particle with a) R_p = 160 nm and b) R_p = 300 nm at short distances with I = 0.01 *M* for different surface charge densities (σ).

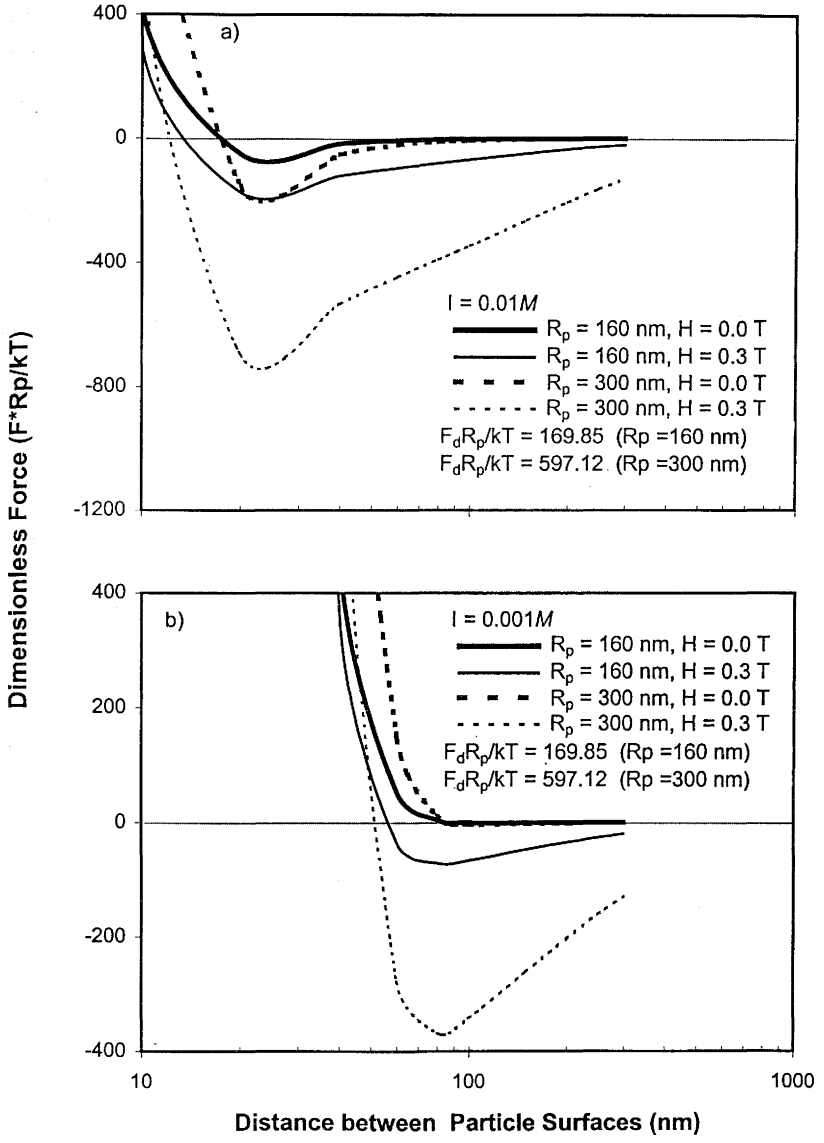

FIGURE 11. Net dimensionless force (Pe) between magnetite (R_s = 400 nm) and plutonium particles of two different sizes, under different magnetic field conditions, with $\sigma = 0.01$ C/m^2, and (a) I = 0.01 *M* and (b) I = 0.001 *M*.

In both cases, the magnetic forces were longer ranged and became more important than the electrostatic forces for separations larger than about 20 nm for the 0.01 *M* case and 90 nm for the 0.001 *M* case. The range over which the electrostatic force became nonexistent was also independent of the charge density, and it depended more importantly on the electrolyte concentration. Even at applied magnetic fields as low as 0.3 T, the strength of the magnetic force was still very long ranged, attracting plutonium particles from relatively large distances. Furthermore, in the breakthrough experiments, the interstitial velocity was so low that large boundary layers were expected. Therefore, the actual drag force was expected to be markedly smaller than the values shown in the figures. In conclusion, even when the electrostatic forces were very strong and impeded the particles of intermediate paramagnetic properties (plutonium and americium) from touching the surface of the magnetite particles, magnetic forces were longer ranged and strong enough to hold plutonium or americium particles in stable positions in the proximity of the magnetite particle without being affected by the viscous force. This stabilization of magnetite particles in an externally applied magnetic field was likened to a similar phenomenon associated with magnetically stabilized fluidized beds (32).

Comparison with Nonmagnetic Batch Processes

Traditionally, ferrites have been used effectively for actinide removal, but usually in a batch mode in the absence of a magnetic field. For example, Slater et al. (33) recently investigated the use of magnetite in an ex situ, batch, nonmagnetic process at pH 12 for the removal of plutonium from wastewater. This process was referred to as ex situ because magnetite was added to the water to effect separation. Figure 12 gives a comparison between the batch results of Slater et al. (33) and the breakthrough results from this work (see Figure 6) in terms of the magnetite loading as a function of the solution concentration.

It must be emphasized that the comparison between these batch and flow processes was generally very difficult for the following reasons. First, the batch results could not simply be scaled to the MPE column results because of the limited data that were available: No batch data were available in the region of the flow results. Second, the concentrations of plutonium in solution corresponded to the final concentrations for the batch process, whereas for the continuous flow process, they corresponded to the feed

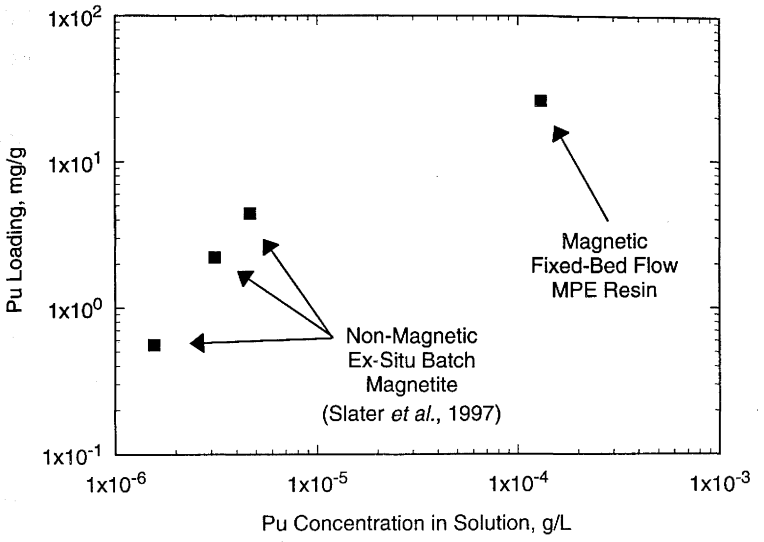

FIGURE 12. Comparison between loading results from the MPE resin using a 0.3-T magnetic field (results from Figure 6) and some nonmagnetic ex situ batch experiments with no magnetic field (33).

concentration. Nevertheless, it was intriguing that the MPE resin exhibited significantly higher loadings (a factor of 5 or so) as compared with the ex situ results of Slater et al (33). In fact, the MPE resin exhibited a loading that was beyond the monolayer metal-ion adsorption capacity of magnetite, which is around 15 mg/g, based on the surface site density of magnetite being 5 sites/nm^2 (34) and considering a surface area of 7 m^2/g. But most importantly, metal-ion adsorption via surface complexation did not appear to be the main removal mechanism with the MPE resin, which showed immediate and marked release of plutonium when the magnetic field was turned off (see Figure 8), indicating an HGMS effect.

CONCLUSIONS

The use of a new magnetic adsorbent material in a fixed-bed mode surrounded by an electromagnet was shown to be very efficient for the removal of plutonium and

americium from wastewater. This material, called magnetic polyamine-epichlorohydrin (MPE) resin, is spherical and nonporous and has activated ferrite particles attached to the outer surface. In this form, the magnetite freely retained the actinide species of interest, while the interstices between the beads promoted good flow-through properties in a fixed-bed mode.

The MPE resin was used to demonstrate a new separation process concept that couples the principles of HGMS with surface complexation (metal-ion adsorption). Experimental results carried out with plutonium and americium in pH 12 wastewater and in the presence of an externally applied magnetic field of 0.3 T showed a dramatic increase in the magnetite capacity as compared with results in the literature that did not utilize an external magnetic field.

A theoretical analysis of the experimental results qualitatively substantiated the experimental findings in terms of a magnetic heteroflocculation model that accounted for magnetic, van der Waals, electrostatic, viscous, and Brownian forces. Since both species are known to form colloidal nanoparticles at pH 12, this model showed that the principal mechanism for removal of the paramagnetic species, plutonium and americium, from wastewater was associated with the high magnetic field gradients created by the magnetite particles. The magnetic force dominated the process, even with the relatively low magnetic field strength (0.3 T) that was used, and for the small and only weakly paramagnetic particles of plutonium and americium that were present.

ACKNOWLEDGEMENTS

The authors gratefully acknowledge financial support from the National Science Foundation, under Grant CTS-9520897, and from Laidlaw Environmental Services, Inc., in the form of a Graduate Fellowship to A.D.E.

REFERENCES

1. E. G. Kelly and D. J. Spottiswood, *Introduction to Mineral Processing*, John Wiley & Sons, New York, 1982.
2. J. H. P. Watson in *Solid-Liquid Separation: High Gradient Magnetic Separation,* Third Edition, L. Svarovsky, Ed., Butterworth-Heinemann, Oxford, 1990.

3. A. M. H. Shaikh and S. G. Dixit, Water Res. *26*, 845 (1992).
4. L. R. Avens, L. A. Worl, K. J. de Aguero, F. C. Prenger, W. F. Stewart, D. D. Hill and T. L. Tolt, "Environmental Remediation using Magnetic Separation", paper presented at the AIChE Annual Meeting, Miami Beach, Florida, November, 1992.
5. S. Miltenyi, W. Muller, W. Weichel, and A. Radbruch, Cytometry *11*, 231 (1990).
6. G. Bitton, G. F. Gifford, and O. C. Pancorbo, Removal of Viruses from Water by Magnetic Filtration, Report PB-261494, U.S. NTIS, 1976.
7. R. R. Dauer and E. H. Dunlop, Biotechnol. Bioeng. *37*, 1021 (1991).
8. C. Tsouris and T. C. Scott, J. Colloid Interface Sci. *171*, 319 (1995).
9. C. Tsouris, S. Yiacoumi, and T. C. Scott, Chem. Eng. Commun. *137*, 147 (1995).
10. C. Tsouris, T. C. Scott, and M. T. Harris, Sep. Sci. Technol. *30*, 1407 (1995).
11. S. Yiacoumi, D. A. Rountree, and C. Tsouris, J. Colloid Interface Sci. *184*, 477 (1996).
12. C. Tsouris and S. Yiacoumi, Sep. Sci. Technol. *32*, 599 (1997).
13. R. L. Kochen and J. D. Navratil, Removal of Radioactive Materials and Heavy Metals from Water Using Magnetic Resin, U.S. Patent 5,595,666 (1997).
14. R. L. Kochen and J. D. Navratil, Method for Regenerating Magnetic Polyamine Epichlorohydrin Resin, U.S. Patent 5,652,190 (1997).
15. R. L. Kochen and J. D. Navratil, Lanthanide/Actinide Res. *2*, 9 (1987).
16. R. L. Kochen, Actinide Removal from Aqueous Solution with Activated Magnetite, Report RFP-4100, Rockwell International, Rocky Flats Plant, Golden, Colorado, 1987.
17. T. E. Boyd and R. L. Kochen, Ferrite Treatment of Actinide Waste Solutions: Continuous Processing of Rocky Flats Process Waste, Report RFP-3476, Rockwell International, Rocky Flats Plant, Golden, Colorado, 1993.
18. T. E. Boyd, M. J. Cusick, and J. D. Navratil, in *Recent Developments in Separation Science: Ferrite Use in Separations Science and Technology,* Vol. VIII, CRC Press, Boca Raton, Florida, 1986.
19. J. D. Navratil, "Metal Recovery and Waste Processing Using Ferrites", EPD Congress Proceedings, TMS, Pennsylvania, 1990, p. 125.
20. A. D. Ebner, J. A. Ritter and H. J. Ploehn, Sep. and Pur. Technol. *11*, 199 (1997).
21. C. A. Feldt and G. T. Kekish, Weakly Basic Anion Exchange Resins, US Patent 3,092,617 (1963).

22. N. V. Blesing et al., in *Ion Exchange in the Process Industries: Some Ion-Exchange Processes for Partial Demineralization,* Society for Chemical Industry, London, 1979.
23. A. D. Ebner, J. A. Ritter and H. J. Ploehn, J. Colloid Interface Sci., submitted (1998).
24. H. C. Hamaker, Physica *4*, 1058 (1937).
25. R. Hogg, T. W. Healy and D. W. Furstenau, Trans. Faraday Soc. *62*, 1638 (1966).
26. G. T. Seaborg, J. J. Katz and W. M. Manning, *The Transuranium Elements*, Vol. 14 B, Part I, McGraw-Hill Co., Inc., New York, 1949.
27. J. Davis and J. O. Leckie, J. Colloid Interface Sci. *74*, 32 (1980).
28. J. Davis and J. O. Leckie, J. Colloid Interface Sci. *67*, 90 (1978).
29. J. Davis, R. O. James and J. O. Leckie, J. Colloid Interface Sci. *63*, 480 (1978).
30. L. E. Katz and K. Hayes, J. Colloid Interface Sci. *170*, 477 (1995).
31. A. P. Robertson and J. O. Leckie, J. Colloid Interface Sci. *188*, 444 (1997).
32. V. I. Sikavitsas, R. Yang, M. A. Burns, and E. J. Langenmayr, Ind. Eng. Chem. Res. *34*, 2873 (1995).
33. S. A. Slater, D. B. Chamberlain, S. A. Aase, B. D. Babcock, C. Conner, J. Sedlet, and G. F. Vandegrift, Sep. Sci. Technol. *32*, 127 (1997).
34. H. Tamura, E. Matijevic, and L. Meites, J. Colloid Interface Sci. *92*, 303 (1983).